

BEP: Bit Error Pattern Measurement and Analysis in IEEE 802.11

Jiayue Li*, Zimu Zhou*, Chen Zhang[†], Liang Yin[†] and Lionel M. Ni[‡]

*Department of Computer Science and Engineering, Hong Kong University of Science and Technology

[†]School of Information and Communication Engineering, Beijing University of Posts and Telecommunications

[‡]Department of Computer and Information Science, University of Macau

{jliay, zzhouad}@cse.ust.hk, zhangcbupt@gmail.com, yinl@bupt.edu.cn, ni@umac.mo

Abstract—The IEEE 802.11 is a set of Media Access Control (MAC) and Physical Layer (PHY) specifications which concern the Wireless Local Area Network (WLAN) service. However, most IEEE 802.11 WLAN services are easily affected by external elements, such as the homogeneous interference caused by the high-density deployment of IEEE 802.11 devices, the attenuation effect caused by complicated indoor obstacles, and the heterogeneous interference caused by other devices which operate out of unlicensed 2.4GHz ISM bands. In this paper, we first present a method to capture IEEE 802.11n Bit Error Patterns (BEP) under the network effect such as the homogeneous interference and the signal attenuation caused by obstacles. We separate the two issues by showing the specific BEP distributions under different channel conditions. In addition to the IEEE 802.11n BEP analysis, we further simulated the impact of the LTE-Unlicensed (LTE-U) signal to the IEEE 802.11ac at the 5GHz, and analyzed similar BEPs through a purely experiment based method.

Keywords: IEEE 802.11n, PHY, Legacy Mode, IEEE 802.11ac, LTE-U, BEP, Channel State Information.

I. INTRODUCTION

Wireless Local Area Networks (WLAN) are prevalent in our lives. We share messages from WLANs everyday by connecting with the access point. Unlike a wired cable network, we have to deploy routers to make sure that users from dynamic areas can receive good and steady quality signals from a specific WLAN. However, wireless signals are easily to be impacted by dynamic factors, such as the distance, the obstacle, and unknown interferers.

Wi-Fi, or IEEE 802.11 standards, is one of the most popular WLAN service. Despite its popularity, it is usually a tough task to maintain good Quality of Service (QoS) for Wi-Fi networks. Since Wi-Fi services operate at part of the unlicensed Industrial, Scientific, Medical (ISM) band, various wireless networks, such as Bluetooth and ZigBee, would coexist and gather at this frequency band. Even the microwave oven can induce interference at this frequency band [1]. In addition to interferences from heterogeneous and homogeneous devices [2], [3], Wi-Fi networks also suffer from dynamic network issues including the inefficient Carrier Sense Multiple Access with Collision Avoidance (CSMA/CA) [4], [5] scheme and severe attenuation from obstacles such as walls and furniture, all of which can lead to bad QoS. The past years has witnessed massive research on addressing these network

issues experimentally. Yet a pre-requisite for these solutions is to first accurately identify the specific network issue that leads to bad QoS. That is, given a specific WLAN that suffers bad QoS, can we diagnose the exact network causes to such bad QoS in real-time?

Previous studies [6]–[8] have explored the method to detect the bad impact from the nearby networks, which mainly focused on the signal interference. However, their methods need to construct a purely new scheme to detect and quantify these bad impacts, which is advanced but costly and function limited. Some further studies focused on analyzing the deep transmission elements, such as the Signal-to-Noise Ratio (SNR) and the Received Signal Strength Indication (RSSI). Although these parameters could reflect the real channel conditions, it is not so accurate [9] by simply measuring the fluctuations under different effects, such as the interference or the signal attenuation.

The LTE-U is also brought into our study, and it is actually the LTE signal operates at the unlicensed band. Some organizations^{1, 2} have already evaluated the possibility of supporting the LTE service at the 5GHz unlicensed band. As the IEEE 802.11ac is operating at the 5GHz band, the possible heterogeneous interference might be generated when they are coexisting at the same local area. Thus, we wish to utilize the similar method to present the specific BEPs based on these two kinds of communications.

In our study, we will present a particular method to measure and define the bit-level error patterns under different network effects, including the homogeneous signal interference, and the signal attenuation caused by the obstacle. The bit error comes from the bits which eroded during the transmission. With the logical modification of the physical layer inside the IEEE 802.11n scheme, the bit error in each frame could be captured. By showing the specific BEPs in dynamic channel conditions, we could accurately recognize the exact network problem we are suffering. Furthermore, the pattern analysis combined the CSI as one of the parameters to quantify the dynamic channel conditions. Additionally, with the advanced software based simulation devices and the similar pattern analysis, we could

¹LTE Advanced in Unlicensed Spectrum C Qualcomm: <https://www.qualcomm.com/invention/technologies/lte/unlicensed>

²U-LTE: Unlicensed Spectrum Utilization of LTE C Huawei: www.huawei.com/ilink/en/download/HW_327803

further achieve the BEP discovery between the IEEE 802.11ac and LTE-U signals, which is another attached fresh study.

The main contributions are summarized as follows:

- 1) We measured and identified three notable BEPs from the real effects of the homogeneous interference and the attenuation after we analyzed the PHY scheme of the IEEE 802.11n Legacy Mode. It is easy to be manipulated and achieves low overheads.
- 2) We combined fine-grained CSI data to show the distribution of the BEPs under the dynamic channel conditions.
- 3) We further simulated the heterogeneous interference between the IEEE 802.11ac and the LTE-U signal with a pure experimental based design. Additionally, we identified the BEPs from this simulation work and showed the pattern distributions under the communications with dynamic bandwidth and signal strength.

II. BACKGROUND

This section first reviews the necessary background for common network issues such as the interference and the attenuation effects for popular WLANs at the 2.4GHz ISM band. Then, we introduce the IEEE 802.11n frame body we utilized. Finally, we review the coexistence of the IEEE 802.11ac and the LTE-U at the 5GHz band and the channel state information.

A. The Interference and the Attenuation Effect

Interference and attenuation are two classic network issues at the 2.4GHz ISM band. Our study mainly focuses on the homogeneous interference caused by the IEEE 802.11 overlapping signals and the attenuation effect due to the obstacles. As shown in Figure 1, there are at most three non-overlapping channels for current 2.4GHz band. The same color represents the non-overlapping channels, and the homogeneous interference is mainly caused by the nearby overlapping channels or the other objects operates at the same channel. In our study, we manipulated the homogeneous interference by operating two kinds of communications at the same channel.

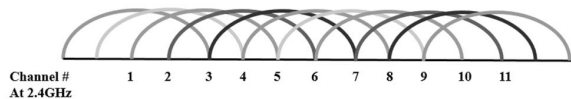


Fig. 1. All 11 channels at 2.4GHz ISM Band

The wireless signal, such as emits from the router is easy to be affected by the nearby obstacles (Figure 2). We could analyze the indoor attenuation effect caused by the obstacles and the distance. Five routers were deployed at specific locations, and their nearby places showed a good quality of signal strength which represented with the color of green. With the impact from the walls or other objects, the signal was attenuated, and the color was turned from green to yellow or even red. The attenuation is one of the possible effects leads to the bad quality of service, just like the homogeneous interference. However, the solutions for both



Fig. 2. Attenuation Effect



Fig. 3. 802.11n WLAN frame, Legacy Mode

effects are distinct. For interference problem, we usually pay more attentions on the signal cooperation. On the other hand, the attenuation effect is more concerning about the signal coverage. Thus it is important to identify the problem that we are suffering and find the suitable solution to improve the QoS.

B. The Frame Body of IEEE 802.11n

The IEEE 802.11n is one of the Media Access Control (MAC) and Physical Layer (PHY) specifications inside the family of IEEE 802.11. Comparing with other standards such as the 802.11a/b/g, the IEEE 802.11n is an improved version. This standard achieves a better data transmission rate and throughput at the 2.4GHz ISM band. In our experiment, we achieved the PHY modified IEEE 802.11n transmission based on the USRPs and manipulated a hotspot as the interferer which also operated under the same standard. Figure 3 is the OFDM format of the Legacy Mode. This mode supports the transmission with a 20MHz channel, and our experiment is based on this format. The 20MHz channel is separated into 64 subcarriers, and the subcarriers -21, -7, 7 and 21 are utilized for pilot signals. Based on our modifications, we didn't modify the Legacy-Short Training Field (L-STF), Legacy-Long Training Field (L-LTF) and Legacy-Signal Field (L-SIG), because our purpose is to check the frame data which eroded by the effect of the interference or the attenuation. Hence, our modifications are focusing on the fourth partition, the data field. The data field contains the service field, the user data and the tails, the modified partition is the user data. According to the data frame inside the data field, we set the frame length with 1000 Bytes, and we defined a thousand 8-bit contents. Thus, all we need is to compare all the contents we sent and received. For each frame, it could show different kinds of BEPs from the eroded contents. With the support of the Channel State Information (CSI) data, we could further recognize the distributions of specific patterns under different kinds of channel conditions.

C. The coexistence of IEEE 802.11ac and LTE-U

Comparing with the IEEE 802.11n, the IEEE 802.11ac is another updated version with the differences at the MAC and PHY specification, which supports the utilization of at the 5GHz. Though there are several similar characters based on their frame format, the IEEE 802.11ac scheme is more complicated. Long-Term Evolution (LTE) technology is another popular standard which supports a relatively high-speed data transmission based on the current wireless communications, such as the mobile phone. For current 4th generation LTE scheme, unlike the LTE service at the licensed band, some researchers have evaluated the possibility of operating the LTE communication at the unlicensed (LTE-U) frequency domain, such as the 5GHz band. Thus, the coexistence of the IEEE 802.11ac and the LTE-U will possibly bring the similar heterogeneous interference just like the IEEE 802.11 and IEEE 802.15.4 at the 2.4GHz ISM band. According to our experiment, since the LTE-U communication is still not opened to the audience, we choose to simulate the interference between the IEEE 802.11ac and the LTE-U inside a pure experimental based method. The BEP is also discovered from the signal we generated, and it is meaningful to capture the differences of these patterns under different channel conditions.

D. Channel State Information

The Channel State Information (CSI) represents the channel condition in a specific wireless communication. The properties such as the fading, scattering, and power decay with distance could be described by the CSI. Since it characterizes channel diversity in the frequency domain, CSI has been adopted to improve the performance of wireless communications and networking [10]–[12]. In our study, we collected the CSI data simply to represent the different channel conditions. With the reasonable quantification of the channel conditions, we will analyze the distributions of the specific BEP under both the interference and the attenuation effects.

III. PATTERN DEFINITION

In this section, we will first introduce the content in each frame, and then define three notable BEPs under the interference and the attenuation. Finally we will combine the CSI data to identify the specific distributions of the subcarriers module value under different effects.

A. Bit Error in the Contents

This subsection introduces the detailed measurement settings. For each data frame, its size is 1000 bytes, with 1000 one-byte contents. For each content, we transmit it as a decimal number and it can be represented as an 8 bits binary message. Thus, the bit errors in each content can be calculated from the hamming distance between the defined 8-bit content and the 8-bit content we received, after the effect of the interference and the attenuation. We use XOR to obtain all bit errors in a whole frame, and we defined another principle to determine whether the frame is correctly received.

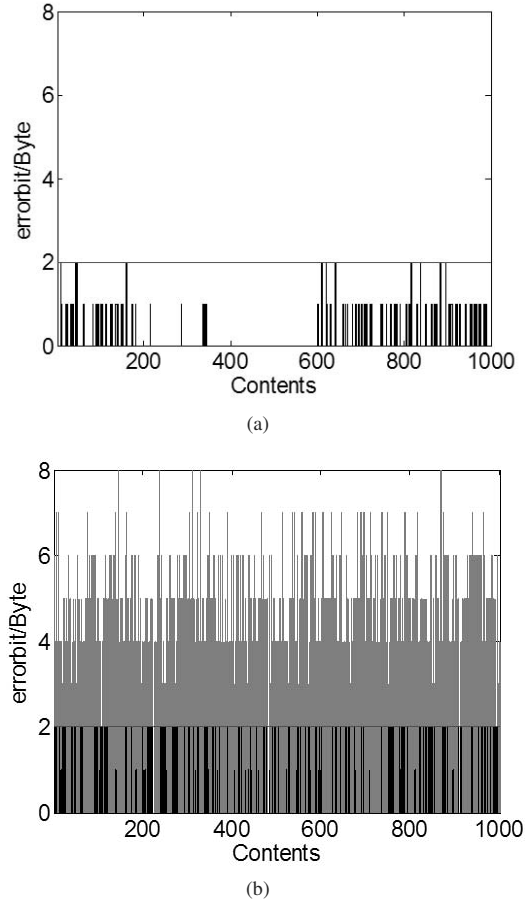


Fig. 4. The packets which are received (a) and lost (b)

Among these 1000 contents for each frame, if one of the content shows an error with more than two bits, the whole frame will be treated as lost. We show two kinds of frames which successfully received and lost from Figure 4. We colored the hamming distance as black when there are no more than two bits error in each content, and the red represents the hamming distance is more than two bits error. With the modifications inside the GNURadio, we record both the received and lost frames. All frame data may exhibit specific BEPs according to specific frame.

B. Preliminary Patterns

Before showing the error patterns, we first define several functions and symbols. For each frame F , as we have defined each content C as an 8-bit binary number before we transmit, we compare the received content C^* with XOR and count the bits which are changed.

For each k -th content, the amount of the bit errors equals to $\text{Count}(C_k \oplus C_k^*)$, where $k \in \{1, 2, 3, 4, 5, \dots, 1000\}$.

1) Correct-Received Patterns

According to this kind of pattern, when there exists a frame F_i (i -th frame for all frame data we transmit) which all of its 1000 contents (8000 bits) are correct,

without any bit errors, then we could define this kind of pattern as the **correct-received pattern** (Figure 5).
 $\text{Count}(C_k \oplus C_k^*) = 0$, for all k from 1 to 1000.

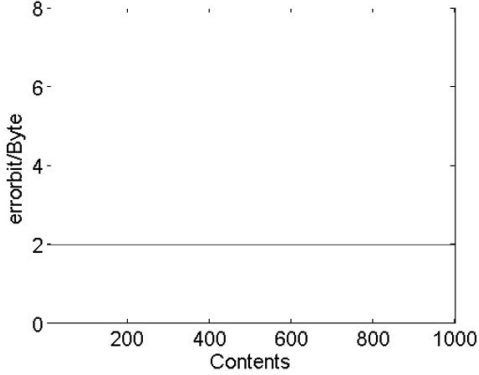


Fig. 5. Correct-Received Pattern

2) Received Patterns

According to this kind of pattern, when there exists a frame F_i which none of its specific content has more than two bit errors, and it is not the **correct-received pattern**, then we could define this kind of pattern as the **received pattern** (Figure 6).

$\text{Count}(C_k \oplus C_k^*) \leq 2$, for all k from 1 to 1000.

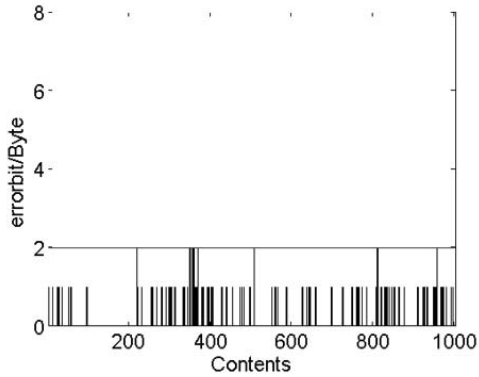


Fig. 6. Received Pattern

3) Lost Patterns

Comparing to the top two kinds of patterns which showed the patterns of the frame has been successfully received, the lost pattern is concerning about the frame which we define it is lost during the transmission. If there exists a frame F_i which at least one of its content has more than two bit errors, then, we defined this kind of frame as the **lost pattern** (Figure 7).

There exists at least one received content C_k^* , where $\text{Count}(C_k \oplus C_k^*) \geq 3$, for all k from 1 to 1000.

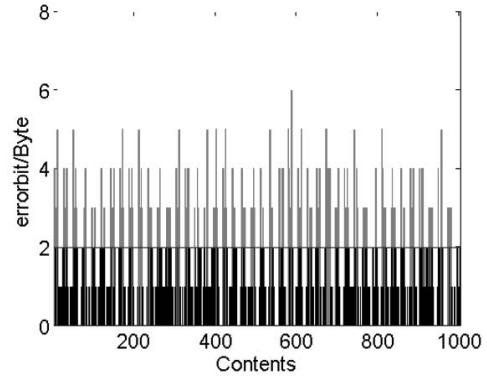


Fig. 7. Lost Pattern

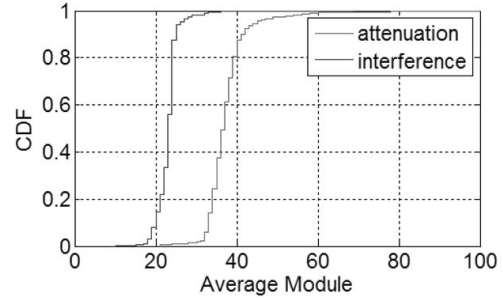


Fig. 8. The CSI distributions under two effects

C. Different Channel Conditions

In the last subsection, we showed three preliminary patterns under interference and attenuation. In this subsection, we will present the distribution of the specific CSI module value distributions under different effects. According to the mapping between the 46 subcarriers and the frame data, we calculate the module value from each 46 subcarriers to quantify the impact from the frame we transmit. Based on the fluctuation of the subcarriers module, it shows distinct distributions under different network effects (Figure 8): For each subcarrier, the data is collected with a complex number, and we calculate the module for each of them. Then we obtain the average module by combining all 46 subcarriers. In Figure 8, the X-axis represents the average module, and the Y-axis shows the cumulative distribution of different module under both effects. For each average module, it will map to at least one frame data we transmitted. Later, we will analyze the percent of the specific BEPs based on these dynamic average module values.

IV. EXPERIMENTAL SETTINGS AND ANALYSIS

A. Hardware Devices And Software Supports

Our experiments are mainly separated into two partitions, one main part is at the 2.4GHz ISM band, and another concerns about the simulations of the interference between the IEEE 802.11ac and the LTE-U signals. In the first partition, we

set two USRP N210 as the transmitter and the receiver. Both USRP devices are equipped with the RFX2450 daughterboard. Except for the USRP devices, we employed two laptops as the interferer by building an Ad-hoc network. One of the laptop operated as the hot spot, which could spread the signal to another laptop. In the second partition, to simulate the interference between IEEE 802.11ac and the LTE-U, we employed the Agilent device MXG N5182B as the signal source and the PXA N9030A as the spectrum analyzer (Figure 9).

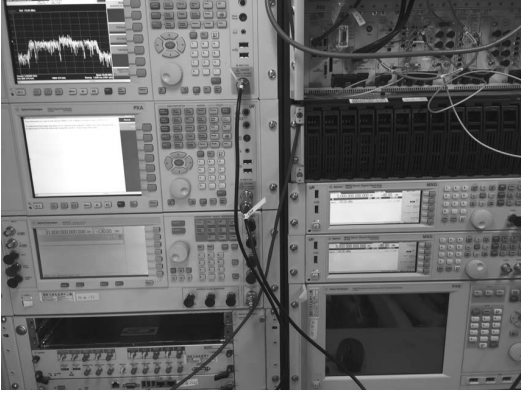


Fig. 9. All Agilent devices we utilized

For software supports in our experiments, we utilized the GNURadio in the first partition study, which is a software based development toolkit. With the help of the GNURadio, we modified the format of the data frame inside the PHY, which achieved the specific transmission under the scheme of the IEEE 802.11n. In order to scan the utilization of different channels at the 2.4GHz ISM band, an IEEE 802.11 network discovery tool, the NetSurveyor was employed during our experiment. In the second partition, the simulation of the interference between the signal of the IEEE 802.11ac and the LTE-U was achieved to modulate with the SystemVue.

B. Experimental Environment

To construct the effect of the interference, we first set our hardware devices in an indoor office with line-of-sight transmission. The effect of attenuation was constructed in another indoor office with sufficient obstacles. With the support of the NetSurveyor, we could detect that there are multiple access points providing IEEE 802.11n services near both offices, and they usually operate at the 1st, 6th, and the 11th channel. Inside this office, we could construct the normal interference effect with the Ad-hoc network which we build with two laptops, and the USRPs are close enough to this Ad-hoc network. In the second experiment, as this experiment mainly simulated the interference effect with a pure software based architecture, its experimental environment does not need to be special picked.

C. Detailed Analysis

In this subsection, we will present the detailed deployment and the analysis of our experiments separately. In the first and

the second partitions, we would try to analyze the effects of the interference and the attenuation inside an IEEE 802.11n network. Thus, we would firstly describe the experimental deployment in both effects. On the other hand, we would bring the regression analysis to show the distributions of different kinds of patterns we have defined. The distinct pattern distributions could be observed from both results under the effect of the interference and the attenuation.

According to the third partition, we would show the process of how we simulated the interference between the IEEE 802.11ac and the LTE-U signals. Additionally, as we recorded the bit error in this simulation, the BEP analysis was attached at the same time.

1) *Interference Effect*: The interference in our first partition experiment is settled as an effect caused by the signal collisions between the same standard. In our experiment, we constructed an Ad-hoc network operated under the IEEE 802.11n. Except for the network we built, we made a deep observation of the nearby radio frequency signals, because we want to null the bad interference effect from other channels. The USRPs would operate at the same channel as the Ad-hoc network did. The channel selection is a tough work, because as we were searching the nearby RF signals, we observed that there were at most four access points providing the IEEE 802.11n services. Fortunately, after we located the center frequencies of each access point with the Netsurveyor, we found that all access points were mainly operating at three non-overlapping channels, the 1st, the 6th, and the 11th channels. Furthermore, there was no other IEEE 802.11 signal source operating at the adjacent channels of the 1st, 6th or 11th. Hence, before we start to generate the interference to the USRPs transmission, we could firstly make sure that there was no any other interferer nearby.

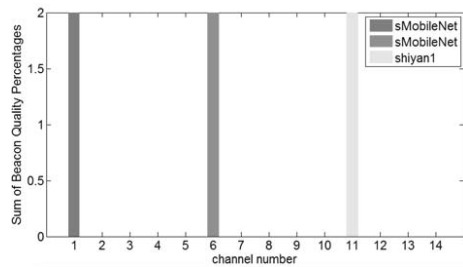


Fig. 10. Nearby network observations under the interference effect

In Figure 10, we could also notice that our Ad-hoc network was operating at the 11th channel, and there was no interferer at the adjacent channels. Different colors represent different networks, and the height of each bar shows the beacon quality, the right bar represents the network we have built. These results are all obtained from the NetSurveyor.

After we finished the deployment of the Ad-hoc network, we maintained the transmission inside this network. As there was one laptop acting as the hotspot, another laptop would download the specific files from this hotspot, which made this

channel busy. The deployment of the USRPs is similar as the Ad-hoc network. We employed two USRPs inside the Ad-hoc network, and let them communicate at the same channel with the Ad-hoc network. We modified the frame data inside the PHY with the GNURadio. Based on these two USRP devices, we constructed a similar IEEE 802.11n transmission, and we manipulated the specific frame to transmit between the both sides. Within this modification, we set the frame size as the 1000 Bytes and transmit 1 Mbytes for each time. The QPSK modulation scheme was adopted. To achieve the interference between these two networks, we recorded the data when both networks are busy concurrently. As we have already defined the frame content before we transmit, we could check the differences between the frame we received and we send. There are total of 8000 bits for each frame, and we could obtain the specific number of bit errors by doing XOR calculations.

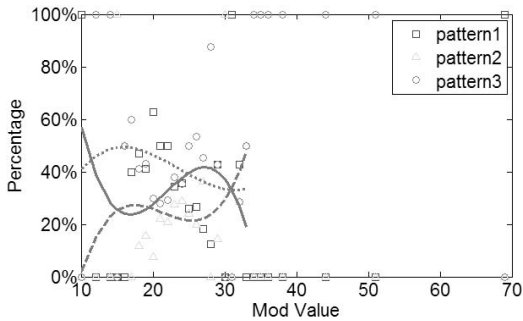


Fig. 11. BEP under the interference effect with dynamic channel conditions

As in Figure 11, we present the percentage of the BEP under the effect of the interference with dynamic channel conditions. According to our statistic work, the 46-subcarrier modules are distributed in the range from 10 to 69, and almost 80 % of the frames' modules gathered at around 15 to 33. We defined this domain as the cluster. Just for record, some modules might only map to a single frame and showed 100 percent distributions on a specific pattern. Furthermore, some modules are too far away from the cluster. Thus, we choose to ignore them during our pattern analysis.

2) *Attenuation Effect*: The attenuation in our first partition experiment is settled as another effect caused by the obstacle. We construct a non-line-of-sight transmission between our USRP devices. Compared to the interference effect, which we set the transmission as the line-of-sight, we will add the obstacle inside this experiment. Similar to the last one, we would first set the communication between two USRP devices without any interferer. However, we simply need to utilize the NetSurveyor again to find a clean channel to avoid any bad external interference to our USRP transmission. As in Figure 12, there were three access points nearby, and two of them were operating at the 1st channel, and another was operating at the 11th channel. Thus, we could set our USRP to operate at the third non-overlapping channel, in this case, the 6th channel.

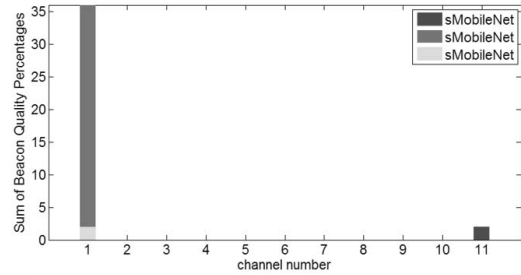


Fig. 12. Nearby network observations under the attenuation effect

After we nulled the possible interferer from the nearby scenario, we set one of the USRP as the transmitter to send the same frame as the interference experiment, and let another USRP to receive the frame with a non-line-of-sight transmission. After the transmission of all 1 Mbytes frames, we analyze the BEP from the received frame. The checking process is similar as the interference pattern analysis. We perform XOR between the frame sent and received.

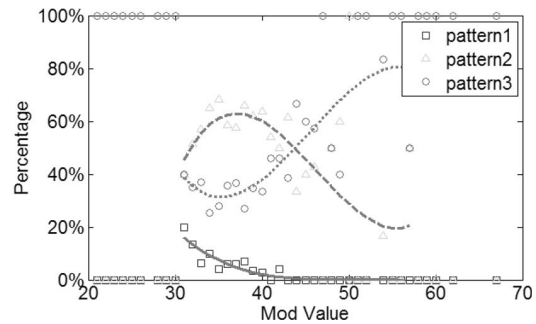


Fig. 13. BEP under the attenuation effect with dynamic channel conditions

In Figure 13, we present the percentage of the BEP under the effect of the attenuation with dynamic channel conditions. The 46-subcarrier modules are distributed in the range of 21 to 269, and the cluster is almost ranged from 31 to 57. We also nulled the modules which their distributions are staying at 100 percent for a specific pattern during our detailed analysis.

3) *Heterogeneous Interference At 5GHz Band*: We generated the 802.11ac signal by using the SystemVue software. We occupied a bandwidth of 40MHz by aggregating two 20MHz bands and sent it to a Keysight MXG. Since the purpose of our simulation is to study the interference between the Wi-Fi and LTE-U signals, we manipulated the signal to transmit at 5GHz. We used another MXG to send an LTE signal whose bandwidth can be chosen to be either 10MHz or 20MHz. Then we combined the two signals through a combiner, and output to two PXA by using a divider. One PXA showed the spectrum and the other sent the baseband signal to PC for demodulation and BER calculation. For further analysis, we separately recorded the bits from source and receiver by using a sink model. Thus, the BEPs could be obtained from the

specific frames as the previous experiment.

According to our simulations, we analyzed the distribution of the bit error amounts from 0 to 8 under four kinds of LTE-U signal interferences. These four kinds of signals are constructed with specific bandwidth and RSSI. The bandwidth is defined to be either 10 or 20MHz, and the RSSI is limited at either -40dBm or -50dBm.

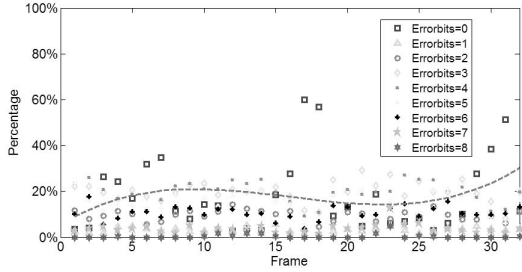


Fig. 14. The error bits distributions under the 10MHz, -40dBm LTE signal

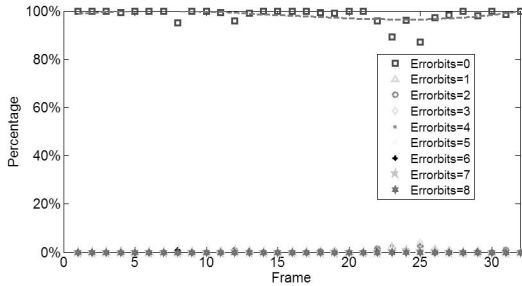


Fig. 15. The error bits distributions under the 10MHz, -50dBm LTE signal

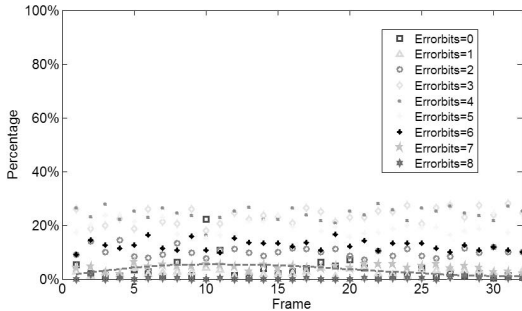


Fig. 16. The error bits distributions under the 20MHz, -40dBm LTE signal

Figure 14 to Figure 17 demonstrate 32 IEEE 802.11ac frames' bit error distributions under four kinds of LTE signal interferences. According to our simulations, the IEEE 802.11ac signal operates with the 40MHz bandwidth and the -40dBm signal strength. Each frame size is 288 Bytes and we could obtain the distributions of the error bits for each frame.

By analyzing these four charts, we observe that when the LTE signal strength is poorer than the IEEE 802.11ac signal,

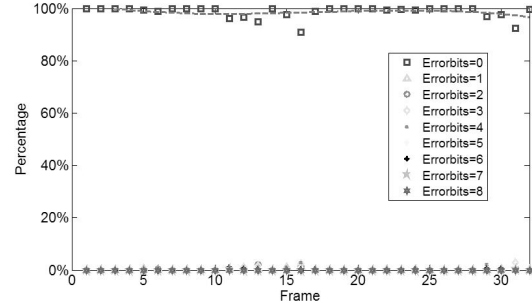


Fig. 17. The error bits distributions under the 20MHz, -50dBm LTE signal

there will be few bit errors based on the IEEE 802.11ac transmission (Figure 15, Figure 17). However, in the case that the LTEs bandwidth is different and the signal strength is the same with the IEEE 802.11ac signal, we could identify the distinct regression result from the 0 error-bit (Figure 14, Figure 16). Thus, in our simulation, we could capture the IEEE 802.11ac error-bit distributions based on the specific LTE interference with distinct bandwidth and signal strength.

V. RELATED WORK

Our work is closely related to the following research. In [13], the authors showed the different patterns of the Chip Error per PN-Code (CEPP) under scenarios such as the interference, the attenuation and the multipath in IEEE 802.15.4 networks. While we utilized a similar way to analyze the BEPs, we focused on the more complex IEEE 802.11n networks, and did not identify the patterns with the bit error and the power level. Conversely, we combined the bit error with the CSI fluctuation, which better showed the connections between the bit error and the specific channel conditions. In addition to the pattern analysis at 2.4GHz, we also extended to the 5GHz band and explore another interference simulation between the IEEE 802.11ac and the LTE-U.

Our work is also relevant to previous research on network measurements and diagnosis in IEEE 802.11 networks. In [14], the authors presented the symbol-error pattern differences of the packet loss caused by the collision or the poor signal strength. In [15], the authors evaluated the in-building wireless network observations of the packet loss rate under interferences and the attenuation caused by the distance and the obstacles. Another link-level research [16] analyzed the effect of the packet loss inside a Roofnet Network, and showed the uniform link errors in a static wireless network. Further, [17] brings the bit error measurements with an IEEE 802.11-compliant radio in an industrial environment.

Most of the research on the LTE-U and the IEEE 802.11ac evaluated the coexistence of these two schemes, such as the throughput analysis and the cooperation between the two [18]–[20]. In this study, we further simulated the heterogeneous interference and try to demonstrate the impact from the LTE-U to IEEE 802.11ac by showing the specific BEPs. We

believe our experimental results are meaningful to quantify the interference level and the bandwidth estimation.

VI. CONCLUSION

In this research work, we first exploited the specific BEPs under the effects of the homogeneous interference and the attenuation in the IEEE 802.11n network. And then, we presented the distributions of the patterns under both effects in the dynamic channel conditions. From the obtained distribution results, we could clearly identify the difference between the effect of the interference and the attenuation. Furthermore, the simulation study based on the IEEE 802.11ac and the LTE-U is attached, and we used the similar method to grab the BEPs under the effect of the heterogeneous interference inside the scenarios of dynamic bandwidth communications.

ACKNOWLEDGEMENT

This research was supported in part by Hong Kong RGC grant HKUST16207714. We thank the State Radio Monitoring Center, Beijing, for their support with the simulation of IEEE 802.11ac and LTE-U communications.

REFERENCES

- [1] R. Gummadi, D. Wetherall, B. Greenstein, and S. Seshan, "Understanding and mitigating the impact of rf interference on 802.11 networks," *SIGCOMM Computer Communication Review*, vol. 37, no. 4, pp. 385–396, 2007.
- [2] X. Zhang and K. G. Shin, "Gap sense: Lightweight coordination of heterogeneous wireless devices," in *Proceedings of IEEE International Conference on Computer Communications (INFOCOM)*, 2013, pp. 3094–3101.
- [3] K. Chebrolu and A. Dhekne, "Esense: Communication through energy sensing," in *Proceedings of ACM Annual International Conference on Mobile Computing and Networking (MobiCom)*, 2009, pp. 85–96.
- [4] S. Sen, R. Roy Choudhury, and S. Nelakuditi, "No time to countdown: Migrating backoff to the frequency domain," in *Proceedings of ACM Annual International Conference on Mobile Computing and Networking (MobiCom)*, 2011, pp. 241–252.
- [5] S. Sen, R. R. Choudhury, and S. Nelakuditi, "Csmacn: Carrier sense multiple access with collision notification," *IEEE/ACM Transactions on Networking*, vol. 20, no. 2, pp. 544–556, 2012.
- [6] S. Rayanchu, A. Patro, and S. Banerjee, "Airshark: Detecting non-wifi rf devices using commodity wifi hardware," in *Proceedings of ACM SIGCOMM Conference on Internet Measurement Conference (IMC)*, 2011, pp. 137–154.
- [7] A. Patro, S. Rayanchu, and S. Banerjee, "Mobicom 2011 poster: Airtrack: Locating non-wifi interferers using commodity wifi hardware," *SIGMOBILE Mobile Computing Communication Review*, vol. 15, no. 4, pp. 52–54, 2012.
- [8] S. Rayanchu, A. Patro, and S. Banerjee, "Catching whales and minnows using wifinet: Deconstructing non-wifi interference using wifi hardware," in *Proceedings of USENIX Conference on Networked Systems Design and Implementation (NSDI)*, 2012, pp. 5–5.
- [9] C. Reis, R. Mahajan, M. Rodrig, D. Wetherall, and J. Zahorjan, "Measurement-based models of delivery and interference in static wireless networks," in *Proceedings of ACM Conference on Applications, Technologies, Architectures, and Protocols for Computer Communications (SIGCOMM)*, 2006, pp. 51–62.
- [10] D. Halperin, W. Hu, A. Sheth, and D. Wetherall, "Predictable 802.11 Packet Delivery from Wireless Channel Measurements," in *Proceedings of ACM Conference on Applications, Technologies, Architectures, and Protocols for Computer Communications (SIGCOMM)*, 2010, pp. 159–170.
- [11] Z. Li, W. Du, Y. Zheng, M. Li, and D. Wu, "From rateless to hopless," in *Proceedings of ACM International Symposium on Mobile Ad Hoc Networking and Computing (MobiHoc)*, 2015, pp. 107–116.
- [12] Z. Li, Y. Xie, M. Li, and K. Jamieson, "Recitation: Rehearsing wireless packet reception in software," in *Proceedings of ACM Annual International Conference on Mobile Computing and Networking (MobiCom)*, 2015, pp. 291–303.
- [13] K. Wu, H. Tan, H.-L. Ngan, Y. Liu, and L. M. Ni, "Chip error pattern analysis in ieee 802.15.4," *IEEE Transactions on Mobile Computing*, vol. 11, no. 4, pp. 543–552, 2012.
- [14] S. K. Rayanchu, A. Mishra, D. Agrawal, S. Saha, and S. Banerjee, "Diagnosing wireless packet losses in 802.11: Separating collision from weak signal," in *Proceedings of IEEE International Conference on Computer Communications (INFOCOM)*, 2008, pp. 735–743.
- [15] D. Eckhardt and P. Steenkiste, "Measurement and analysis of the error characteristics of an in-building wireless network," *SIGCOMM Computer Communication Review*, vol. 26, no. 4, pp. 243–254, 1996.
- [16] D. Aguayo, J. Bicket, S. Biswas, G. Judd, and R. Morris, "Link-level measurements from an 802.11b mesh network," in *Proceedings of ACM Conference on Applications, Technologies, Architectures, and Protocols for Computer Communications (SIGCOMM)*, 2004, pp. 121–132.
- [17] A. Willig, M. Kubisch, C. Hoene, and A. Wolisz, "Measurements of a wireless link in an industrial environment using an IEEE 802.11-compliant physical layer," *IEEE Transactions on Industrial Electronics*, vol. 49, no. 6, pp. 1265–1282, 2002.
- [18] S. S. Sagari, "Coexistence of lte and wifi heterogeneous networks via inter network coordination," in *Proceedings of Workshop on PhD Forum of ACM International Conference on Mobile Systems, Applications, and Services (MobiSys)*, 2014, pp. 1–2.
- [19] A. Bhorkar, C. Ibars, and P. Zong, "On the throughput analysis of lte and wifi in unlicensed band," in *Proceedings of Asilomar Conference on Signals, Systems, and Computers*, 2014, pp. 1309–1313.
- [20] F. Abinader, E. Almeida, F. Chaves, A. Cavalcante, R. Vieira, R. Paiva, A. Sobrinho, S. Choudhury, E. Tuomaala, K. Doppler, and V. Sousa, "Enabling the coexistence of lte and wi-fi in unlicensed bands," *IEEE Communications Magazine*, vol. 52, no. 11, pp. 54–61, 2014.